Biochimica et Biophysica Acta, 1151 (1993) 223–236

BBAMEM 76073

Mitochondrial pyruvate transport in working guinea-pig heart. Work-related vs. carrier-mediated control of pyruvate oxidation

Rolf Bünger [a] and Robert T. Mallet [b]

[a] *Department of Physiology, F.E. Hebert School of Medicine, Uniformed Services University of the Health Sciences, Bethesda, MD (USA) and* [b] *Department of Physiology, Texas College of Osteopathic Medicine, Fort Worth, TX (USA)*

(Received 21 May 1993)

Key words: Myocardium; Pyruvate dehydrogenase; Dichloroacetate; α-Cyanohydroxycinnamate; Mitochondrial pyruvate transporter; Donnan equilibrium

Myocardial pyruvate oxidation is work- or calcium-load-related, but control of pyruvate dehydrogenase (PDH) by the specific mitochondrial pyruvate transporter has also been proposed. To test the transport hypothesis distribution of pyruvate across the cell membrane as well as rates of mitochondrial pyruvate net transport plus oxidation were examined in isolated perfused but stable and physiologically working guinea-pig hearts. 150 μM–1.2 mM α-cyanohydroxycinnamate proved to specifically block mitochondrial pyruvate uptake in these hearts. When perfusate glucose as cytosolic pyruvate precursor was supplied in combination with octanoate (0.2 or 0.5 mM) as diffusible alternative fatty acid substrate, α-cyanohydroxycinnamate produced up to 20- and 3-fold increases in pyruvate and lactate efflux, respectively. Cinnamates did not alter myocardial hemodynamics nor sarcolemmal pyruvate and lactate export. In contrast the tested concentrations of cinnamate produced reversible, dose-dependent decreases in $^{14}CO_2$ production from [1-^{14}C]pyruvate or [U-^{14}C]glucose by inhibiting mitochondrial pyruvate uptake. Linear least-squares estimates of available cinnamate-sensitive total pyruvate transport potential yielded rates close to 110 μmol/min per g dry mass at $S_{0.5} \approx 120$ μM, which compared reasonably well with literature values from isolated cardiac mitochondria. This transport potential was severalfold larger than total extractable myocardial PDH activity of ≈ 32 μmol/min per g dry mass at 37°C. Even when cytosolic pyruvate levels were in the lower physiologic range of about 90 μM, pyruvate oxidation readily kept pace with mitochondrial respiration over a wide range of workload and inotropism. Furthermore, dichloroacetate, a selective activator of PDH, stimulated pyruvate oxidation without affecting myocardial O_2 consumption, regardless of the metabolic or inotropic state of the hearts. Consequently, little or no regulatory function with regard to pyruvate oxidation could be assigned to the native mitochondrial pyruvate carrier of the working heart. Therefore, mitochondrial pyruvate-H^+ symport was the normal, highly efficient (rather than controlling) mechanism for pyruvate entry into the mitochondria where PDH regulation controlled pyruvate oxidation.

Introduction

Pyruvate dehydrogenase (PDH) constitutes a central control point in oxidative energy metabolism in mammalian tissues, especially the myocardium. Thus, PDH catalyzes the essentially irreversible oxidative decarboxylation of pyruvate to acetyl-CoA, and represents the predominant pathway for entry of carbohydrate-derived carbon into the citric acid cycle. PDH is regulated by a complex system of control mechanisms, including feed-back and allosteric regulations by PDH reactants and products and mitochondrial ATP/ADP. Superimposed on allosteric control is covalent activation/inactivation of PDH by phosphatase-catalyzed dephosphorylation and kinase-dependent phosphorylation, respectively [1,2]; this control by interconversion is possibly under the direct influence of mitochondrial Ca^{2+}, which could stimulate the phosphatase, and Mg^{2+} which is required by the kinase. In response to these controls, PDH activity and flux in perfused hearts and isolated mitochondria as well, have been found work- or calcium-dependent, stimulated dose-dependently by catecholamines, and readily adaptable to changing acute myocardial energy expenditures [3–12].

Correspondence to: R. Bünger, Department of Physiology, F.E. Hebert School of Medicine, Uniformed Services University of the Health Sciences, 4301 Jones Bridge Road, Bethesda, MD 20814-4799, USA. Fax: +1 (301) 2953566.

Enzymes: lactate dehydrogenase (EC 1.1.1.27), pyruvate dehydrogenase (EC 1.2.4.1 + EC 1.8.1.4 + EC 2.3.1.12 + EC 3.1.3.43), pyruvate dehydrogenase kinase$_a$ (EC 2.7.1.99), alanine aminotransferase (EC 2.6.1.2), malic enzyme (EC 1.1.1.40), phosphofructokinase (EC 2.7.1.11).

Abbreviations: C_3, three-carbon units; [Pyr], mean concentration of pyruvate (similarly for other metabolites); Ac, acetate; AcAc, acetoacetate; $AcCl_2$, dichloroacetate; Glc, glucose; Lac, lactate; HOB, DL-3-hydroxybutyrate; NE, L-norepinephrine; Oct, octanoate; α-COHC, α-cyanohydroxycinnamate (α-C-3-OHC, α-C-4-OHC, 3-hydroxy and 4-hydroxy congeners, respectively); PDH, pyruvate dehydrogenase complex (PDH_a; PDH_t, active and total form, respectively).

However, complete oxidation of glucose or lactate in the myocardium requires coordinated sarcolemmal and mitochondrial transport prior to end-oxidative degradation by the mitochondria. Obviously a functional cardiac monocarboxylate transport apparatus could be vital for the acute energy balance of the work-loaded heart, especially in severe adrenergic/physical stress where cardiac output and contractility become maximally stimulated. In fact, the possibility has been raised that PDH flux could be restrained by availability of pyruvate in the mitochondrial matrix, due to low pyruvate transporter activity in the inner mitochondrial membrane.

Pyruvate and lactate are natural short-chain aliphatic monocarboxylates, centered at the compartmental interface between cytosol and mitochondria. At low-net glycolytic flux these compounds provide a link between the redox systems and the overall energy status of the myocardium, i.e., the cytosolic phosphorylation potential [13–16]. Cellular and subcellular transport of monocarboxylates can occur by three distinct mechanisms (for review, see Ref. 17): (1) the specific saturable and SH-group-dependent short-chain-monocarboxylate transporter known to exist in mitochondria, red blood cells, Ehrlich ascites cells and likely many other cell types, (2) unspecific non-saturable and SH-independent transport via the anion-exchanger of the cell membrane, a system which has been shown to exist in red cells and hepatocytes, and (3) linear non-ionic diffusion which accounts for movements of the uncharged free acid, likely proceeds via the lipid domain of the cell membrane and is not blocked by inhibitors but instead is strictly related to the pK value of the monocarboxylate. Since pyruvate (pK = 2.49) is virtually completely dissociated at cellular pH ≈ 7.2, the fraction of free pyruvic acid is minute under physiologic conditions and therefore diffusion through the lipid domain of cellular membranes is also minimal. Nevertheless, isolated cardiac mitochondria transport pyruvate at considerable rates at physiologic pH and temperature and this transport is highly sensitive to blockade by α-cyanohydroxycinnamates [18,19].

In the present study an attempt was made to rigorously quantitate the steady state kinetics of pyruvate net transport across the inner mitochondrial membrane in the heart subjected to physiologic workload and inotropic stimulation by catecholamines. As pyruvate transport across the cell membrane proved not seriously affected by sub-millimolar α-cyanohydroxycinnamate concentrations, the blocker effected a Donnan distribution when sufficient amounts of pyruvate were added to the perfusion medium. The specific mitochondrial pyruvate uptake could thus be quantitated from inhibitions by α-cyanohydroxycinnamate of $^{14}CO_2$ production from [U-^{14}C]glucose or [1-^{14}C]pyruvate. Information regarding mechanisms of α-cyanohydroxycinnamate inhibition as well as kinetic characteristics of mitochondrial pyruvate transport was obtained from Dixon- and Lineweaver-Burk-type analyses using linear and nonlinear computer routines [20]. The cytosolic pyruvate concentration required for half maximum mitochondrial uptake as well as the physiologically available maximum net transport potential were also estimated and compared with the published cardiac carrier turnover number or initial transport rates from isolated heart mitochondria [21–24]. This kinetic information combined with data from selective dichloroacetate activations of PDH were used to test the hypothesis [24] that the specific cardiac mitochondrial pyruvate transporter may be rate-controlling for pyruvate oxidation under the intracellular conditions of the working guinea-pig heart. In addition, hearts were stimulated by α- and β-adrenergic agonists during α-cyanohydroxycinnamate blockade to judge the relative importance of the monocarboxylate transporter for the maintenance of myocardial energy balance during physiologic stimulations of ventricular inotropism.

Methods

Isolated working heart perfusions

Hearts were isolated from adult male guinea-pigs (350–450 g body mass) under ether anesthesia. All surgical procedures were performed in accordance with the Guide for the care and use of laboratory animals (NIH publication 85-23, revised 1985). The main physiologic characteristics of the isolated perfused working guinea-pig heart preparation were described previously [7,25]. Hearts were beating at intrinsic sinus rhythm (220–260/min) and performed pressure-volume work under standard hydraulic loads, i.e., at constant preload (left ventricular filling pressure) of 10–12 cmH_2O and constant afterload (mean aortic pressure) of 80–90 cmH_2O.

Perfusion medium was a hemoglobin-free non-recirculating oxygenated (95 : 5 = O_2/CO_2, pH 7.4) modified Krebs-Henseleit solution containing 1.25 mM calcium and 0.6 mM magnesium [16,26]. To minimize endogenous glycogen utilization the medium contained 5 U/l bovine insulin (Sigma, St. Louis, MO); this induced glycogen net synthesis at perfusate glucose concentrations $\geqq$ 1 mM (unpublished observations). Either 0 to 20 mM glucose or 0 to 3 mM pyruvate were the specific metabolic substrates whose oxidation required transporters at both the cell and mitochondrial inner membranes. In all experiments with α-cyanohydroxycinnamates either freely diffusible alternative substrates (acetate (0.5 mM), octanoate fatty acid (0.2 or 0.5 mM)) or transported ketone bodies (DL-β-hydroxybutyrate (5 mM), acetoacetate (2 mM)) were supplied. The diffusible (fatty acid) substrates stabilized

the working hearts both energetically and functionally when the mitochondrial monocarboxylate transporter was disabled by α-cyanohydroxycinnamate. Dichloroacetate (1 or 5 mM) was applied as a selective inhibitor of the PDH kinase in order to maximize the active form of the PDH enzyme complex [27]. Dichloroacetic acid and α-cyanohydroxycinnamatic acid (3-hydroxy or 4-hydroxy congeners) were from Sigma (St. Louis, MO).

Extracellular space

[^{14}C]Mannitol (25–50 μM) or inulin-[^{14}C]carboxylic acid (15 mg/l) were infused for 6 min as extracellular markers [28,29]; arterial and venous specific radioactivities were essentially equal after about 4 min infusion. Extracellular water was taken as the distribution spaces of [^{14}C]mannitol or inulin-[^{14}C]carboxylic acid in stop-frozen myocardium [26,29,30]. The [^{14}C]mannitol and inulin-[^{14}C]carboxylic acid distribution spaces were essentially equal and varied between 0.55 and 0.65 ml/g wet mass. Intracellular water, i.e. total tissue water minus extracellular water, varied between 0.22 and 0.27 ml/g ventricular wet mass or 2.5 to 3.3 ml/g dry mass. For the pyruvate distribution measurements in Table I the critical extracellular spaces were determined in each heart. All ^{14}C-labelled compounds were purchased from Amersham (Arlington Heights, IL).

Parameters measured and principal protocols

Physiologic parameters (heart rate, left ventricular filling and aortic pressures, coronary flow, cardiac output) were monitored [25]. Biochemical and biophysical parameters (O_2, H^+, CO_2, $^{14}CO_2$, metabolites of myocardium and extracellular fluids) were obtained by polarographic (O_2, CO_2), enzymatic (perchloric acid extraction of metabolites), and liquid-scintillation techniques ($^{14}CO_2$ and other ^{14}C-labelled compounds) standard in this laboratory [16,25,30]. Metabolite and radioactivity measurements were corrected for known extraction yields and quenching, respectively [16,25,26, 30]. Released [^{14}C]lactate was isolated, identified, and quantitated as detailed elsewhere [16,31]. Rates of steady-state myocardial uptake or release of monocarboxylates (lactate, pyruvate) were calculated as arterio-venous concentration differences times coronary flow. Perfusions with [U-^{14}C]glucose as precursor of released $^{14}CO_2$ or [^{14}C]lactate were limited to less than 70 min to minimize intracellular label-randomization [31]. The first 20 min of these perfusions were required to establish isotope equilibrium in working hearts exposed to $\geqq$ 1.5 mM [U-^{14}C]glucose [31]. Validation studies showed that PDH flux measured as $^{14}CO_2$ production from specifically labelled [3,4-^{14}C]glucose agreed well with flux estimates with uniformly labelled [U-^{14}C]glucose. This was verified for radioactive perfusion periods from about 20 min to more than 60 min [31].

A typical radioisotope protocol to measure monocarboxylate transport and oxidation rates in the isolated working hearts follows: (a) 15–20 min post-surgical stabilization period; (b) 12 and 20 min infusion of [1-^{14}C]pyruvate or [U-^{14}C]glucose, respectively, at constant molar specific activity to achieve isotope equilibrium [31]; (c) examination of the effects of α-cyanohydroxycinnamates or dichloroacetate on transport and oxidation alone or in combination with catecholamines. In protocols designed to judge pyruvate transport kinetics at several intracellular pyruvate concentrations, pyruvate, glucose, blockers and catecholamines were infused with step-wise increasing concentrations, each step lasting 16–20 min to establish new functional and metabolic steady states [25].

Data analysis and interpretation of $^{14}CO_2$ production

Quantitative Michaelis-Menten-type information on mitochondrial net transport in working heart could be acquired from rates of $^{14}CO_2$ production only if they were measured at pyruvate concentrations at which pyruvate transport across the mitochondrial membrane was indeed rate-limiting for pyruvate oxidation (PDH flux). For example, the cinnamate compounds produced concentration-dependent inhibition of pyruvate oxidation and hence $^{14}CO_2$ release with [U-^{14}C]glucose as precursor; here the decrease in pyruvate oxidation was secondary to the inhibition of the α-cyanohydroxycinnamate-sensitive mitochondrial transporter. In perfusions with exogenous [1-^{14}C]pyruvate, however, any cinnamate-induced decrease in $^{14}CO_2$ production was an acceptable measure of mitochondrial transport inhibition only if the infused α-cyanohydroxycinnamate concentrations did not seriously limit pyruvate transport across the plasma membrane. Indeed detailed myocardial pyruvate measurements revealed transsarcolemmal Donnan distributions, at least at α-cyanohydroxycinnamate concentrations less than 1.2 mM. Similarly, when dichloroacetate was used to activate PDH [9,27], a secondary increase in mitochondrial pyruvate uptake would indicate that transport was not limiting for decarboxylation.

Also, the rate of myocardial $^{14}CO_2$ release provided a quantitative measure of mitochondrial net transport rate and pyruvate oxidation only if intracellular isotope dilution of the immediate precursor, cytosolic pyruvate, was known or minimal. This was the case in working hearts perfused with labelled glucose in the presence of 5 U insulin/l perfusion buffer, but in the absence of exogenous pyruvate or lactate [31,32]. Similarly, when pyruvate plus insulin instead of glucose plus insulin was added to the perfusion medium in sufficiently high concentrations ($\geqq$ 1 mM pyruvate), $^{14}CO_2$ production from [1-^{14}C]pyruvate quantitatively reflected PDH flux in working guinea-pig heart [5,7]. This was expected since insulin stimulates glycogen synthesis and high

perfusate pyruvate concentrations cause citrate accumulation which inhibits glycolytic flux at phosphofructokinase [29,33] and thus minimizes dilution of pyruvate transported into the cell by pyruvate derived from glycogen. However, adrenergic stimulation mobilizes unlabelled glycogen (unpublished observations) which produces a dose-dependent intracellular dilution of labelled pyruvate derived from [U-^{14}C]glucose (cf. Table V, [31]). Thus, in most experiments with catecholamines the specific activity of released lactate was measured to monitor the intracellular specific activity of pyruvate; this was feasible because the perfusion medium did not contain exogenous pyruvate or lactate [31,32].

Michaelis-Menten-type analyses of concentration/effect experiments could be employed to estimate half-maximal effective substrate concentrations ($S_{0.5}$) for pyruvate net transport (plus oxidation), assuming the concentration-rate curves were rectangular hyperbolic and the limiting mechanism obeyed simple Michaelis-Menten kinetics according to $v_o = V_{max} \cdot [S]/(K_m + [S])$. However, the present analysis does not reveal the true K_m or unidirectional V_{max} of the transport protein. Nevertheless, the steady state kinetics provided information about the physiologically available net flux or transport characteristics under conditions of ventricular hydraulic work.

Statistics and fitting non-linear equations

Data are presented as single values or as means ± S.E. Single comparisons of means were accomplished by Student's *t*-tests; if not stated otherwise, *P* values refer to one-tail *t*-tests. Multiple comparisons were accomplished by analysis of variance (ANOVA) in combination with Tukey's procedure to control the experimentwise error [34]. R^2 was the proportion of variability in the dependent variable that is explained by the independent variable. $P \leqq 0.05$ was considered significant.

Data plotted according to Dixon (titrations with variable α-cyanohydroxycinnamate at constant perfusate pyruvate concentrations) were subjected to three-stage linear least-squares analysis using Gaussx and Gauss software, versions 2 (Aptech Systems, Kent, WA); this procedure allows estimations of a system of linear equations, thus adequately accounting for the

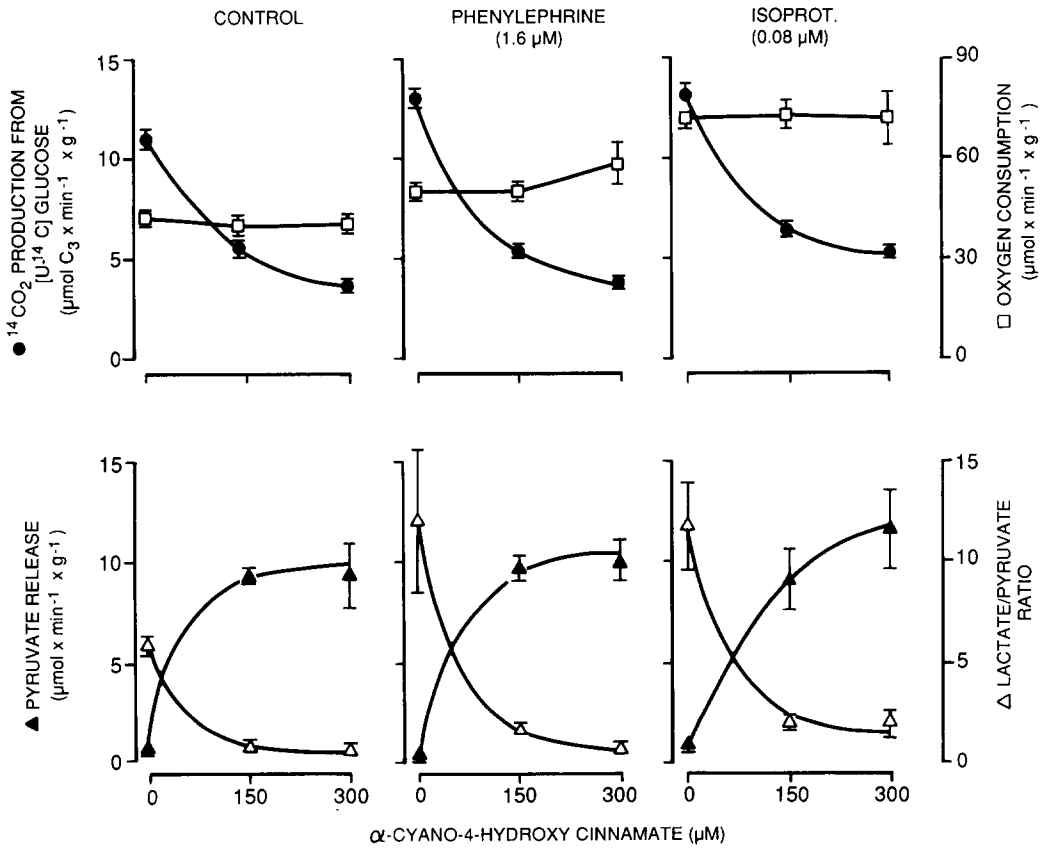

Fig. 1. Inhibition of glucose oxidation and massive pyruvate export induced by α-cyano-4-hydroxycinnamate in the absence and presence of adrenergic agonists. Working hearts were energetically and hemodynamically stablized by 0.2 mM octanoate as diffusable alternative fatty acid substrate. To minimize intracellular dilution of labelled pyruvate from [U-^{14}C]glucose, perfusate glucose concentration was raised to 15 mM in presence of 5 U/l insulin. Metabolic rates, expressed as μmol C_3/min per g dry mass, refer to steady states attained after 16–20 min in presence of α-cyano-4-hydroxycinnamate and the catecholamines, respectively. Values are means ± S.E., $n = 4$–6, from the last 3 min of each experimental phase (control, catecholamine, 150 μM cinnamate, and 300 μM cinnamate).

overall data scatter and variance/covariance of the residuals when coefficients and standard errors are computed. For example, in a Dixon-type titration protocol the effects of various α-cyanohydroxycinnamate concentrations at 1 mM vs. 2.5 mM pyruvate were fitted simultaneously. On the other hand, in Lineweaver-Burk-type analyses (titrations with variable pyruvate concentrations at constant α-cyanohydroxycinnamate levels), the regression coefficients were obtained assuming non-linear rectangular hyperbolic saturation kinetics and fitting the equation with non-linear maximum likelihood routines. The following general non-linear form instead of the classical linear double reciprocal plot was used:

$$\text{rate} = \text{concentration}/(\alpha \cdot \text{concentration} + \beta) \qquad (1)$$

where $1/\alpha$ = maximum possible rate for a given condition, β = rate constant (slope in double reciprocal depiction), $S_{0.5} = \beta/\alpha$ (concentration at which rate = 0.5 maximum rate). The major advantage of this non-linear equation compared to the Lineweaver-Burk plot is that the non-linear form is defined for zero substrate conditions and also for negative rates, e.g., when net uptake is replaced by net release at low to zero perfusate substrate concentrations. Thus, the rates measured at zero precursor concentrations could be included in the analysis, which markedly improved the precision of the fits. Further, the maximum-likelihood method, unlike the non-linear least-squares analysis, is not based on the assumption of a normal distribution of observations and is therefore more generally applicable to obtain good estimates of coefficients and standard errors in statistical models [20,34]. In the non-linear model (Eqn. 1), regression coefficients ± S.E. values were iteratively estimated using first the Gauss algorithm and in the final iteration the Bernd-Hall-Hall-Hausman algorithm [16,20]; this produced correct S.E. values for the estimated coefficients.

Results and Discussion

Massive myocardial pyruvate export due to α-cyano-4-hydroxycinnamate and adrenergic agonists

Fig. 1 depicts the effects of α-adrenergic (phenylephrine) and β-adrenergic stimulation (isoproterenol)

TABLE I

Effects of α-cyanyhydroxycinnamtes and dichloroacetate on myocardial pyruvate distribution and pyruvate-linked cytoplasmic intermediates in perfused working guinea-pig heart utilizing external carbohydrates

Values are means ± S.E., $n = 4$–8, from working hearts (see Materials and Methods) perfused for 30 min followed by freeze-clamping the myocardium. Negative, positive transsarcolemmal pyruvate net flux denotes myocardial release (export), uptake (import), respectively. αC-4-OHC, α-cyano-4-hydroxycinnamate; αC-3-OHC, α-cyano 3-hydroxycinnamate; Glc, glucose; Oct, octanoate; Ac, acetate; Pyr, pyruvate; $AcCl_2$, dichloroacetate; $[Pyr]_i$, mean intracellular pyruvate concentration; $[Pyr]_e$, mean intracoronary pyruvate concentration = 1/2·(arterial [Pyr]+ venous [Pyr]; pH_1 = intracellular pH according to Ref. 15; calculated pH_i, $((-\log([H^+]_a/[H^+]_v))/2 - \log([Pyr]_i/[Pyr]_o))$.

Series	Condition	μM			pH_i		μmol/g dry mass		Transsarcolemmal pyruvate net flux (μmol/min per g dry mass)
		$[Pyr]_i$	$[Pyr]_e$	$[Lac]_i$	measured	calculated	Malate	Alanine	
I	5 mM Glc	93 ±15	5 ±0.5	377 ±68	7.212 ±0.003	–	0.21 ±0.03	2.60 ±0.15	−0.27 ±0.03
II	5 mM Glc + 0.5 mM Oct	154 ±34	4 ±0.4	915 ±144	7.194 ±0.009	–	0.34 ±0.12	3.56 ($n = 2$)	−0.65 ±0.13
III	5 mM Glc + 0.5 mM Oct + 0.17 mM αC-4-OHC	595 ±136	66 ±8	1879 ±300	7.186 ±0.003	–	0.93 ±0.09	11.70 ±0.89	−5.78 ±0.84
IV	5 mM Glc + 0.5 mM Oct + 0.86 mM αC-3-OHC	666 ±61	70 ±7	1946 ±230	7.180 ±0.005	–	0.88 ±0.21	–	−6.79 ±0.83
V	5 mM Glc + 0.5 mM Ac	132 ±20	6 ±3	1120 ±104	7.214 ±0.003	–	0.21 ±0.03	2.36 ($n = 1$)	−0.89 ±0.13
VI	5 mM Glc + 0.5 mM Ac + 1 mM $AcCl_2$	36 ±11	4 ±0.8	1170 ±174	7.221 ±0.010	–	0.23 ±0.01	1.41 ±0.18	−0.48 ±0.11
VII	1 mM Pyr + 0.5 mM Oct	369 ±24	887 ±13	1155 ±195	7.211 ±0.004	6.960 ±0.030	0.72 ±0.06	9.76 ±0.06	13.40 ±1.21
VIII	1 mM Pyr + 0.5 mM Oct + 1.2 mM αC-3-OHC	684 ±47	980 ±20	1680 ±315	7.221 ±0.005	7.214 ±0.032	0.70 ±0.11	11.42 ±0.91	1.8 ±0.60
IX	1 mM Pyr + 0.5 mM Ac	296 ±40	923 ±38	1858 ±359	7.214 ±0.004	6.887 ±0.063	0.71 ±0.08	7.23 ($n = 2$)	12.58 ±1.80
X	1 mM Pyr + 0.5 mM Ac + 0.86 mM αC-3-OHC	731 ±48	952 ±14	2430 ±243	7.216 ±0.005	7.267 ±0.031	0.48 ±0.09	8.66 ±0.20	3.66 ±1.44

on glucose oxidation and pyruvate export from α-cyano-4-hydroxycinnamate-treated working hearts perfused with 15 mM [U-^{14}C]glucose plus 0.2 mM octanoate. Octanoate prevented cardiac failure due to α-cyanohydroxycinnamates which occurred with glucose or pyruvate as the sole substrate (unpublished observations). In control working hearts (Fig. 1, left panels) α-cyano-4-hydroxycinnamate concentrations between 150 to 300 μM greatly increased (up to 20-fold) myocardial pyruvate release in association with 50% inhibition of $^{14}CO_2$ production from labelled glucose. In contrast, cinnamate did not change myocardial O_2 consumption (Fig. 1, upper left panel) or cardiac work parameters (not shown), as octanoate was present as alternative substrate. Lactate release also increased in these cinnamate-treated hearts [31] but less than pyruvate. Therefore the lactate/pyruvate ratio in coronary effluent decreased during α-cyanohydroxycinnamate infusion (Fig. 1, lower left panel).

Myocardial O_2 consumption increased only slightly with 1.6 μM phenylephrine and more markedly with 0.08 μM isoproterenol. Both adrenergic agonists stimulated $^{14}CO_2$ production from labelled glucose about 20% (Fig. 1, upper middle and right panels). However, the catecholamines did not attenuate the efficacy of α-cyanohydroxycinnamate as an inhibitor of glucose oxidation and stimulator of pyruvate release. These effects of α-cyano-4-hydroxycinnamate were dose-dependent. Again O_2 consumption (Fig. 1, upper middle and right panels) and cardiac work (not shown) were not changed. Obviously, catecholamine stimulation of the non-failing, octanoate-stabilized working hearts did not alter dose-dependent inhibition of mitochondrial pyruvate oxidation nor stimulation of myocardial pyruvate export by α-cyanohydroxycinnamate. In agreement with Halestrap [21] these observations are difficult to reconcile with the concept of adrenergic hormonal control of the mitochondrial pyruvate carrier. The observations also made clear that α-cyano-4-hydroxycinnamate doses which strongly blocked the mitochondrial monocarboxylate transporter, effected marked increases, not decreases, in pyruvate export from the hearts. This demonstrated that monocarboxylate transport at the sarcolemma of the guinea-pig heart was not seriously impaired by α-cyano-4-hydroxycinnamate.

Re-distribution of pyruvate across the sarcolemma due to α-cyano-3(or 4)-hydroxycinnamate

Evidence that α-cyano-3-hydroxycinnamate, up to 1.2 mM did not disable sarcolemmal pyruvate transport in the guinea-pig heart is presented in Table I. In a first series of experiments hearts were perfused with glucose and octanoate as substrates. As predicted from Fig. 1 intracellular and extracellular pyruvate concentrations increased 4-fold and nearly 20-fold, respectively, due to the α-cyanohydroxycinnamates when hearts utilized glucose (Table I, series III, IV). The α-cyanohydroxycinnamates induced only minor decreases in intracellular pH. However, major pyruvate-linked cytosolic metabolites, lactate (lactate dehydrogenase), alanine (alanine-aminotransferase), and malate (malic enzyme), accumulated due to the cinnamate-induced intracellular accumulation of pyruvate.

In a second series of experiments with 1 mM exogenous pyruvate and octanoate or acetate as substrates (Table I, series VII–X), cytosolic lactate and alanine levels were again greatly increased by α-cyano-3-hydroxycinnamate. However the main effect under these conditions was the nearly 2-fold accumulation of cytosolic pyruvate ($P < 0.01$). Of special interest, during cinnamate infusion, the intracellular pyruvate approached but did not exactly equal the extracellular perfusate concentration ($P < 0.05$). Nevertheless, since myocardial pyruvate uptake was more than 70% diminished (low net flux conditions according to last column of Table I, series VIII, X), the tissue appeared to be close to equilibrium with respect to pyruvate distribution across the cell membrane. This conclusion was consistent (1) with Fig. 1 where cinnamate treatment did not noticeably impair monocarboxylate export, and (2) with Table I series VIII and X, where myocardial pyruvate net uptake was reduced to less than 10% of the maximum rate near 40 μmol/min per g dry mass as previously determined [29].

Sarcolemmal pH gradient

If membrane pyruvate transport was essentially H^+-symport [35,36], the observed pyruvate distribution during α-cyanohydroxycinnamate blockade could reflect the prevailing pH-gradient (Donnan equilibrium) across the sarcolemma according to the following relationship [17,35]:

$$\log([Pyr]_i/[Pyr]_o) = pH_i - pH_o = \Delta pH \qquad (2)$$

In fact, close inspection of the pH data of Table I reveals that measured pH_i [15] and pH_i calculated assuming Donnan equilibrium ($-\log([H^+]_a/[H^+]_v])/2 - \Delta pH = pH_{i,calc.}$) are in good agreement during α-cyanohydroxycinnamate treatment of the pyruvate-perfused hearts. In the untreated pyruvate hearts $pH_{i,calc.}$ appeared to underestimate pH_i by about 0.3 pH units ($P < 0.01$). This disparity most likely resulted from the large net pyruvate uptake by these control hearts, 13 μmol/min per g dry mass (Table I, series VII, IX). This rate is > 30% of the maximum sarcolemmal uptake capacity in the guinea-pig heart [29] and appeared to be sufficient to produce non-equilibrium distribution of pyruvate across the plasma membrane (Table I, series VII, IX).

These results also help better define the plasma membrane pH gradient in the working heart. From Table I it seems clear that the normal pH gradient must be relatively small, near 0.1 pH unit, as the mean extracellular pH is about 7.3 at $pH_a \approx 7.4$ and $pH_v \approx 7.2$ in the perfused working hearts [15,37]. A > 0.4 pH unit gradient was reported for guinea-pig cardiomyocytes cultured in citrate-buffer [38]. A 0.4 pH gradient for the present working hearts would require intracellular bicarbonate levels near 60 mM because the Krebs-Henseleit bicarbonate level was 25.5 mM. However, measured intracellular bicarbonate concentrations in both blood-perfused and Krebs-Henseleit perfused hearts are 3-fold lower, 19–20 mM [13,15]. The present pH_i estimates based on pyruvate equilibration or intracellular HCO_3^-/CO_2 ratios [15] are in good agreement with a number of recent ^{31}P-NMR estimates of pH_i (7.16–7.22) in isolated guinea-pig [39–41] and ferret hearts [42].

Selective α-cyanohydroxycinnamate inhibition of pyruvate uptake by native mitochondria

According to Fig. 1 and Table I, quantitative characterization of mitochondrial pyruvate uptake using α-cyanohydroxycinnamate treatment was feasible, since cinnamate up to 1.2 mM did not seriously disturb sarcolemmal pyruvate transport. In a separate series of experiments it was shown that glucose oxidation ($^{14}CO_2$ production) and pyruvate export increased in parallel when perfusate [U-^{14}C]glucose was raised from 1.5 to 10 mM. This occurred without any increase in O_2 consumption and only minor increases in the specific radioactivity of cytosolic pyruvate as monitored by released [^{14}C]lactate ($n = 5$–7, data not shown). Consequently, the concentration dependence of in situ mitochondrial pyruvate transport and oxidation at constant mitochondrial respiration could be assessed between 1 and 20 mM [U-^{14}C]glucose. Fig. 2 shows glucose oxidation as a function of perfusate glucose concentration and the dose-dependent inhibition of mitochondrial $^{14}CO_2$ production from [U-^{14}C]glucose by α-cyano-4-hydroxycinnamate. Even at very low levels of perfusate [U-^{14}C]glucose, 1.5 mM, the mean relative specific activity of released [^{14}C]lactate was 0.45 ± 0.002 ($n = 8$) at 0, 100, 200, and 300 μM α-cyano-4-hydroxycinnamate. Because 2 mol lactate are produced per mol glucose in glycolysis, thus lowering molar specific activity 50%, these data indicate only minimal intracellular dilution of pyruvate derived from infused [U-^{14}C]glucose plus 5 U/l insulin [31].

Fig. 2 also shows that the maximum oxidation rates were decreased in presence of α-cyano-4-hydroxycinnamate when perfusate glucose and hence cytosolic pyruvate were varied within normal limits. This inhibition pattern was consistent with either reversible noncompetitive inhibition or a reversible mixed-type mechanism (nomenclature according to Refs. 43 and 44). Requisite reversibility of the cinnamate inhibition was demonstrated in short-term 16-min infusions of 150 μM ($n = 4$–7), 300 μM ($n = 3$), or 600 μM ($n = 3$) α-cyano-4-hydroxycinnamate. In these experiments, increased external carbohydrate concentrations (either in the form of glucose or pyruvate) could neutralize the inhibitory effects of the submaximal cinnamate doses, and pyruvate oxidation returned to control rates within 4 min after termination of cinnamate infusion.

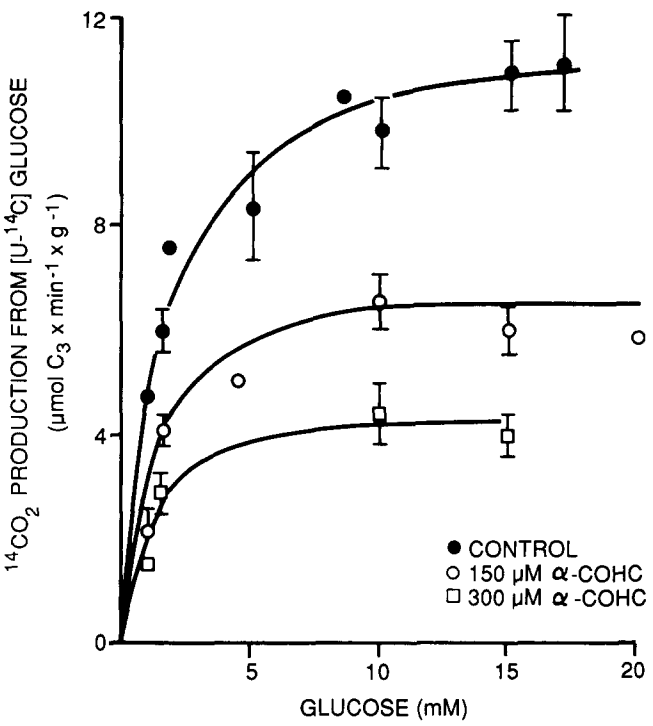

Fig. 2. Concentration-dependence of glucose oxidation in working hearts stabilized with 0.2 mM octanoate and effects of α-cyano-4-hydroxycinnamate. After establishment of isotope equilibrium within 20 min [31] the arterial concentration of [U-^{14}C]glucose was step-wise increased at constant specific activity ($\approx$ 3000–5000 dpm/μmol), each step lasting 8 min. α-Cyano-4-hydroxycinnamate was infused to the concentrations indicated only after isotope equilibria were established at the lowest glucose concentrations tested (1.0–1.5 mM). Rates (μmol C_3/min per g dry mass) are means from the last three minutes at each concentration. $^{14}CO_2$ production was not corrected for the specific activity of lactate; however, because 5 U/l insulin was infused intracellular dilution of pyruvate was minimal or essentially absent even at the low to normal (1.5–5.0 mM) [U-^{14}C]glucose concentrations (Table V, [31]). Data are means ± S.E., $n = 4$–6, or single values.

However, the predominant inhibition mechanism for α-cyanohydroxycinnamate appeared to be non-competitive. This became evident when the α-cyanohydroxycinnamate concentrations were varied in presence of two different but constant pyruvate concentrations. The results (Fig. 3) from four such titration experiments using step-wise increases of α-cyano-3(or 4)-hydroxycinnamate from 200 to 1200 μM are depicted in the form of Dixon plots. Interestingly, the measured

TABLE II

Regression parameters of linear semi-reciprocal fits (Dixon plot) of the effects of α-cyano-4-hydroxycinnamate on $^{14}CO_2$ production from [1-^{14}C]pyruvate by perfused working guinea-pig heart stabilized by 0.2 mM octanoate

Fitted parameters are means (±S.E.) and measured values are steady state triplicate measurements from the cinnamate infusions of Fig. 3. *N*, number of input data points from linear portions of Dixon plots, i.e., the control rates measured prior to cinnamate infusion were not included in the fits. [a] Fits obtained by staged least-squares analyses (see Materials and Methods) using all the data from the two pyruvate conditions in presence of cinnamate. Perfusate cinnamate concentrations were measured by UV absorbance at $\lambda = 340$ nm and converted to intracellular concentrations assuming distribution according to sarcolemmal pH gradient derived from measured pH_o and pH_i. Fitting the inhibited rates ($n = 16$) from the infusions of the 3-hydroxy congener according to Fig. 3 yielded similar yet not identical results: the intersections on ordinate were different ($P < 0.01$) and those on abscissa were nearly different ($P = 0.06$), a pattern appropriately termed mixed inhibition. * $P < 0.05$ relative to 1 mM pyruvate condition; n.s., not significantly different.

Conditions [1-^{14}C]Pyruvate (mM)	*N*	Intersection on ordinate [a]		Intersection on abscissa [a] (fitted, μM)	Fitted maximum rate (μmol/min per g dry mass)	Mechanism of inhibition
		fitted	measured			
1	4	0.286±0.59	0.45	−64±14	35	non-competitive
2.5	4	0.090±0.089 *	0.33	−36±37 (n.s.)	111	

individual control rates for pyruvate oxidation, obtained prior to infusion of the cinnamates (reciprocals of the ordinate values in Fig. 3), were consistently lower than the control rates graphically extrapolated from the respective linear portions of the cinnamate-inhibited rates. This was confirmed by least-squares estimates of the cinnamate-sensitive control rates which are compared with the measured control rates in Table II, 'intersection on ordinate'. A plausible explanation for the disparities between measured and extrapolated control rates could be that basal pyruvate transport rate increased due to cinnamate-induced intracellular pyruvate accumulation (see Table I). The magnitude of this effect is indicated by extrapolating the pyruvate transport rates to zero-inhibitor concentration.

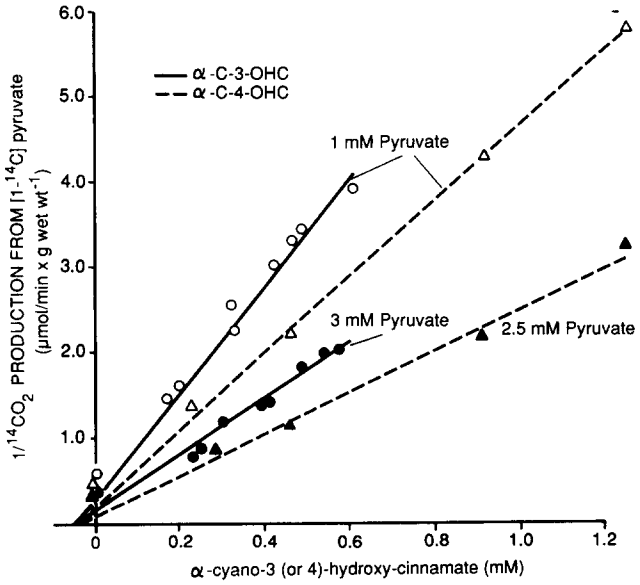

Fig. 3. Non-competitive inhibition of myocardial pyruvate oxidation by submillimolar concentrations of α-cyanohydroxycinnamates. Graphic analysis (Dixon plot) of pyruvate oxidation versus intracellular α-cyanohydroxycinnamate concentration in working guinea-pig hearts utilizing 1 or 2.5 to 3 mM [1-^{14}C]pyruvate plus 0.2 mM octanoate. $^{14}CO_2$ production rates are means from triple determinations at the steady states attained after 16–20 min step infusions of the α-cyanohydroxycinnamates. Data from six different heart preparations. For further details of the titration protocols and mathematical analyses see Table II.

Quantitative analysis of α-cyanohydroxycinnamate inhibition kinetics

α-Cyanohydroxycinnamate increased intracellular pyruvate but not in a concentration-dependent manner. Consequently inhibition of pyruvate oxidation by α-cyanohydroxycinnamate was suitable for a Dixon-type least-squares regression analysis. The analysis was further improved by taking into account the known instantaneous sarcolemmal pH gradients * and the fact that poorly metabolizable weak acids like the cinnamates distribute across the sarcolemma according to the pH gradient. Thus, measured extracellular α-cyanohydroxycinnamate concentrations were used to estimate intracellular concentrations by substituting cinnamate into Eqn. 2. The Dixon plots of Fig. 3 are based on intracellular cinnamate concentrations.

The data of Fig. 3 were fitted by paired linear least-squares routines (see Materials and Methods) to obtain more accurate estimates of the intersections on ordinate and negative abscissa (K_i). The regression coefficients for the α-cyano-4-hydroxycinnamate experiments are presented in Table II. The results confirmed that the mechanism of the 4-hydroxy congener was predominantly non-competitive in the heart. This was evident because the intersections on the abscissa were not significantly different at 1 mM or 2.5 mM

* pH gradients derived from measured arterial, venous and intracellular pH according to Materials and Methods.

pyruvate plus blocker ($P = 0.25$). Thus, the intracellular K_i for non-competitive inhibition by 4-hydroxycinnamate was about 50 μM.

Inhibition by the 3-hydroxy congener also was curvilinear with a similar Dixon plot as that seen with the 4-hydroxy congener (Fig. 3). However, there were distinct quantitative differences: the intersections on the negative abscissa were very nearly different (one-tail $P = 0.06$) at 1 mM vs. 3 mM pyruvate (not shown). This data suggested the more complex pattern of mixed inhibition [43,44]. It remained however unclear at this stage of the study, whether the inhibition by the 3-hydroxy congener was of a competitive/non-competitive type or whether competition was not involved at all, i.e., whether the mechanism was non-competitive/uncompetitive.

Concentration-dependent oxidation of pyruvate

The concentration-dependence of pyruvate oxidation was studied by varying exogenous pyruvate concentrations in the absence of cinnamate. Non-linear estimates of maximum oxidation rates were compared with extractable PDH activity published previously [5–7]. Perfusate pyruvate was step-wise increased between 0.8 mM and 3.0 mM. A rectangular hyperbolic relationship (saturation kinetics) between concentration and pyruvate transport plus oxidation was assumed. Eqn. 1 was fitted using $^{14}CO_2$ production rates and intracellular pyruvate concentrations by employing the non-linear maximum likelihood routines (see Methods). Regression coefficients ± S.E. and R^2 values for such hyperbolic fits are compared for three different control conditions in Table III: series I (octanoate, no catecholamine), series III (octanoate plus norepinephrine), and series V (catecholamine, no octanoate). As expected, estimated maximum pyruvate oxidation rates increased from 17 to 30 μmol/min per g dry mass ($P < 0.01$, series I, III), when the octanoate-perfused hearts were stimulated by a large dose of norepinephrine (0.2 μM) which is known to activate PDH flux to a near-maximum of 32 μmol/min [5,6]. When octanoate was omitted from the perfusion medium (to minimize negative feedback) and pyruvate was the sole substrate during norepinephrine stimulation, estimated maximum rate increased to 25 μmol/min per g dry mass (Table III, series I vs. V; $P < 0.01$). This latter rate corresponded to a PDH_a/PDH_t ratio of ≈ 0.8, in close agreement with the previously reported 75–80% PDH_a activity in norepinephrine-stimulated working hearts utilizing 1 mM pyruvate as sole substrate [5,6].

In the absence of octanoate dichloroacetate maximized conversion of native PDH into the active form

TABLE III

Regression parameters of rectangular hyperbolic (saturation-type) fits of the effects of [1-^{14}C]pyruvate on $^{14}CO_2$ production in presence of constant concentrations of α-cyano-hydroxycinnamates and dichloroacetate, respectively

Fitted parameters are means (± S.E.) or single values; N, number of input data points from the metabolic steady states in the pyruvate titrations including zero values prior to [1-^{14}C]pyruvate infusion. Each fit is based on data from 2–4 hearts. Rates expressed as μmol/min per g dry mass. Octanoate was 0.2 mM in series III, IV and 0.5 mM in series I, II. To obtain a good estimate of the maximum physiologic pyruvate oxidation rate, working hearts were stimulated by norepinephrine (NE) in presence of dichloroacetate ($AcCl_2$) but in the absence of octanoate (series VI). R^2, correlation coefficient which explains the percent variability in the dependent variable ($^{14}CO_2$ production); $S_{0.5}$, pyruvate concentration for half maximum rate. V_{max}, fitted maximum rate. [a] Fit based on mean extracellular pyruvate concentration. [b] Fit based on estimated intracellular pyruvate concentration (see Text). For other abbreviations see legend to Table I. * $P < 0.02$ relative to respective control; n.s., not significantly different.

Series	Condition	NE (μM)	N	$1/V_{max}$ (fitted)	V_{max}	R^2	Slope (fitted)	$S_{0.5}$ (mM)	Mechanism
A. [1-^{14}C]Pyruvate oxidation in presence of octanoate									
I	Control	–	10	0.0583 ±0.0012	17.2	0.995	0.0166 ±0.0009	0.12 [b]	non-competitive/competitive
II	0.37 mM αC-3-OHC	–	10	0.1121 * ±0.0055	8.3	0.813	0.1221 * ±0.0071	0.78 [b]	
III	Control	0.2	9	0.0332 ±0.0010	30.1	0.992	0.0114 ±0.0018	0.14 [b]	non-competitive
IV	0.30 mM αC-4-OHC	0.2	9	0.1420 * ±0.016	7.0	0.946	0.0254 (n.s.) ±0.0109	0.13 [b]	
B. [1-^{14}C]Pyruvate oxidation in the absence of octanoate									
V	Control	0.1	10	0.0403 ±0.0043	24.8	0.980	0.0326 ±0.0043	0.81 [a]	max. PDH activation
VI	5 mM $AcCl_2$	0.1	10	0.0309 * ±0.0016	32.4	0.989	0.0189 * ±0.0020	0.61 [a]	

and estimated maximum pyruvate utilization rate increased from 25 to 32 μmol/min per g dry mass (Table III, series V, VI; $P < 0.01$). This estimate was in excellent agreement with total extractable PDH activity at 37°C in the guinea-pig heart [5–7]. Thus, the mathematically fitted rates increased in accordance with expected or published increases in PDH activities, and the absolute maximum decarboxylation potential estimated under conditions of full PDH dephosphorylation (dichloroacetate plus norepinephrine) quantitatively agreed with measured total PDH activity. These results, collectively, suggested that PDH activity, rather than pyruvate transport, was a major controller of pyruvate oxidation. Also in previous studies with calcium- and norepinephrine-stimulated working hearts we observed consistent and parallel changes in PDH activity and PDH flux [5–7].

Concentration-dependent pyruvate oxidation with α-cyanohydroxycinnamate

To assess the potential regulatory role of the mitochondrial membrane pyruvate transporter, arterial perfusate pyruvate concentration was varied at constant α-cyanohydroxycinnamate concentration. In agreement with the cinnamate experiments in Fig. 3, both non-competitive (α-cyano-4-hydroxycinnamate) and mixed (α-cyano-3-hydroxycinnamate) inhibition patterns were observed in these studies. According to Table III, α-cyano-3-hydroxycinnamate strongly reduced the estimated maximum transport plus oxidation rate, from 17 to 8 μmol/min per g dry mass (series I, II). Also the estimated intracellular $S_{0.5}$ ** for pyruvate increased severalfold, from about 120 μM to 800 μM. In addition to the 3-hydroxycinnamate effect on $S_{0.5}$, the slope coefficients (β-parameter in Eqn. 1) were markedly different between control and α-cyano-3-hydroxycinnamate-treated hearts (series I, II of Table III), which ruled out parallel lines in double-reciprocal plots. This excluded an uncompetitive mechanism.

The 3-hydroxycinnamate inhibition pattern (V_{max} decreased, K_m increased) was about halfway between competitive (V_{max} constant, K_m increased) and non-competitive inhibition (V_{max} decreased, K_m constant). Thus the mixed inhibition pattern caused by 3-hydroxycinnamate could be classified as competitive/non-competitive [43,44]. Obviously, the 3-hydroxy congener revealed a distinctive competitive component. Therefore, in general agreement with Halestrap et al. [18] and preceeding work by Paradies and Papa [35], the mechanism of the α-cyanohydroxycinnamates appeared to involve initial competition with pyruvate for entry into the mitochondrial matrix followed by binding to the transport protein at a site different from that of pyruvate. The latter process appeared to establish the dominant non-competitive pattern.

The 4-hydroxycinnamate congener decreased the estimated maximum rate of pyruvate transport plus oxidation from 30 to 7 μmol/min per g dry mass, even in the presence of norepinephrine (Table III, series III, IV). Thus, norepinephrine did not raise estimated maximum rate in the blocked hearts (Table III, series II, IV), which was consistent with Fig. 1 and in sharp but expected contrast to its effect in the untreated controls (Table III, series I, III). Unlike 3-hydroxycinnamate, however, 4-hydroxycinnamate did not raise $S_{0.5}$, regardless of whether intracellular or extracellular pyruvate levels were used in the fitting routines (coefficients for extracellular fit not shown). Consequently, the main effect of the 4-hydroxy congener in concentrations $\geqq 300$ μM was to reduce the amount of functional transport protein, with only minor or no effects on affinity for pyruvate (V_{max} decreased, K_m constant). This clearly shows that α-cyano-4-hydroxycinnamate was a predominantly non-competitive inhibitor of mitochondrial pyruvate transport in the working heart.

Kinetics of physiologic mitochondrial pyruvate uptake

The Dixon-type analyses of Table II were used to assess the physiologically available maximum transport potential of the cinnamate-sensitive transport process in working hearts. This was feasible because of the curvilinear inhibition of transport by cinnamate with no known effects on the PDH complex. The maximum transport potential was computed by linear extrapolation to zero-cinnamate of the appropriate portion of the Dixon plot at 2.5 mM perfusate pyruvate (Fig. 3). The estimate indicated a maximum cinnamate-sensitive rate of about 110 μmol/min per g dry mass (Table II). In similar extrapolations from the titrations with the 3-hydroxy congener (Fig. 3) the estimated maximum rate was ≈ 130 μmol/min. Such large potentials for monocarboxylate transport again imply that PDH, with a 3- to 4-fold lower maximal activity, exerted much greater control over pyruvate oxidation than the specific cinnamate-sensitive mitochondrial carrier.

The estimated maximum transport potential was compared (1) with rates predicted from amount and turnover number of cardiac mitochondrial carrier protein and (2) with V_{max} values derived from initial pyruvate uptake data of Halestrap and colleagues [22–24]. The basis for the first comparison is as follows: heart mitochondrial carrier protein ≈ 290 pmol/mg protein,

** To estimate intracellular $S_{0.5}$ for control hearts, the cellular pyruvate levels were obtained assuming non-equilibrium distribution according to Table I, series VII, and employing measured $[pyruvate]_e$ for each infused pyruvate concentraton; thus intracellular $[pyruvate]_i = 0.42 \times (\text{measured } [pyruvate]_e)$. To estimate intracellular $S_{0.5}$ for the cinnamate-treated hearts, near-equilibrium distribution was assumed according to Eqn. 2 employing measured pH_i, pH_o, and $[pyruvate]_e$, which were obtained for each pyruvate concentration infused.

or 84 nmol carrier protein/g ventricular dry mass, since mitochondrial protein ≈ 290 mg/g dry mass in guinea-pig heart [15,45]. At 6°C, pH 7.0–7.2, the turnover rate was 8/min and 12/min in liver and heart mitochondria, respectively. It increased to 560/min in liver mitochondria at 37°C [22,23]. A similar temperature dependence would give a carrier turnover rate in cardiac mitochondria at pH 7.2 and 37°C of $(12/8) \cdot 560/\text{min} = 840/\text{min}$. At 84 nmol carrier protein/g ventricular dry mass, this value ≈ 71 μmol/min per g dry mass at pH 7.2, 37°C and is of a similar order of magnitude as the present kinetic estimate of 110 μmol/min (Table II, Fig. 3).

The second comparison used transport V_{max} values derived from initial pyruvate uptake rates by isolated heart mitochondria [22,23]. At 6°C, pH 7.2, V_{max} in liver and heart mitochondria were 0.79 and 5.4 nmol/min/mg protein, respectively. At 37°C, pH 7.0, liver mitochondria increased V_{max} to 44.8 nmol/min/mg protein, a 57-fold increase. A similar temperature dependence for heart mitochondria would yield V_{max} at 37°C, pH 7.0, of 305 nmol/min/mg protein. This rate is equivalent to 88 μmol/min per g dry mass for the intact heart. The combined mean of all these estimates is thus near 100 μmol/min per g dry mass, about 3-fold higher than maximal PDH activity.

Dichloroacetate activation of pyruvate dehydrogenase and mitochondrial transport

The substantially larger estimates of pyruvate transport versus maximal PDH activity argue against the notion [22–24] that transport limits pyruvate oxidation. A special series of experiments was designed to directly address this controversy. Dichloroacetate (1 mM) was used to selectively activate PDH [9,46,47]. Dichloroacetate did not affect cardiac work (not shown) nor did it

TABLE IV

Stimulation by 1 mM dichloroacetate of mitochondrial pyruvate transport plus oxidation in perfused guinea-pig heart under various metabolic conditions and adrenergic stimulation

Values are means (±S.E.). Glc, glucose; Oct, octanoate; Pyr, pyruvate; HOB, DL-3-hydroxybutyrate (containing 42% metabolizable D-3-hydroxybutyrate); Ac, acetate; $AcCl_2$, dichloroacetate; AcAc, acetoacetate; NE, norepinephrine; −, not infused; +, infused; * $P < 0.04$ relative to $AcCl_2$-effect in the absence of NE. $^{14}CO_2$ production referred to specific activity of respective arterial radioactive precursor. Hearts performed work under standard load conditions (see Materials and Methods).

Series	Condition	N	Radioactive precursor	$AcCl_2$	NE (μM)	(μmol C_3/min/g dry mass)	
						$^{14}CO_2$ production	mean $AcCl_2$-induced transport rate increase
I	15 mM Glc	3	[U-^{14}C]Glc	−	−	10.7	
	+0.2 mM Oct			+	−	11.3	0.58
II	5 mM Glc	4–8	[U-^{14}C]Glc	−	−	8.3±0.5	
	+0.5 mM Oct			+	−	10.0±0.6	1.82±0.27
				−	0.5	10.3±0.9	
				+	0.5	13.2±1.0	2.86±0.46 *
III	5 mM Glc	2	[U-^{14}C]Glc	−	−	3.5	
	+0.5 mM Oct			+	−	4.9	1.35
	+0.2 mM Pyr			−	0.08	6.0	
				+	0.08	7.0	1.04
IV	1 mM Pyr	2 or 3	[1-^{14}C]Pyr	−	−	9.4	
				+	−	11.3	1.95
				−	0.08	12.9	
				+	0.08	15.0	2.10
V	1 mM Pyr	6	[1-^{14}C]Pyr	−	−	5.8±0.2	
	+5 mM HOB			+	−	7.7±0.3	1.66±0.31
				−	0.08	12.6±0.4	
				+	0.08	15.3±0.8	2.58±0.51
VI	0.2 mM Pyr	3–5	[1-^{14}C]Pyr	−	−	0.9±0.2	
	+5 mM HOB			+	−	2.2±0.3	1.29±0.18
	+1.2 mM Ac			−	0.08	2.0±0.4	
				+	0.08	3.1±0.5	1.06±0.30
VII	0.2 mM Pyr	2	[1-^{14}C]Pyr	−	−	1.4	
	+2 mM AcAc			+	−	2.8	1.36
	+1.2 mM Ac			−	0.08	2.5	
				+	0.08	3.3	0.85

stimulate myocardial (i.e., mitochondrial) respiration. For example, in control and norepinephrine (0.08 μM)-stimulated working hearts which utilized glucose and pyruvate in physiologic concentrations ($n = 7–10$), O_2 uptake (μmol/min per g dry mass) was 40.7 ± 2.7 vs. 37.3 ± 1.9 (dichloroacetate) and 78.1 ± 4.1 vs. 80.0 ± 1.8 (dichloroacetate), respectively.

It was clear that, if mitochondrial pyruvate transport was rate-limiting, pyruvate decarboxylation would not increase at constant mitochondrial respiration in response to dichloroacetate. However, the experimental data were incompatible with this premise. Series I and II of Table IV, for instance, demonstrate that dichloroacetate stimulated pyruvate oxidation by up to 28% when glucose was the precursor in presence of 0.5 mM octanoate and norepinephrine. Under similar conditions with acetate as the alternative substrate it was found that dichloroacetate greatly decreased intracellular pyruvate concentrations (Table I, series VI).

When glucose plus octanoate were combined with physiologic levels of pyruvate (series III of Table IV) dichloroacetate again produced a large stimulation of glucose oxidation (up to 39%). When oxidative metabolic rates were stimulated by norepinephrine under otherwise identical conditions, dichloroacetate further increased $^{14}CO_2$ production from [U-^{14}C]glucose by 17%.

The observed dichloroacetate stimulation of pyruvate oxidation was relatively small when compared with the total PDH activity of about 32 μmol/min at 37°C. However, competing endogenous substrates and perfusate octanoate were always available. Fatty acid and ketone body metabolism exert negative feedback control on PDH flux [4,5,7,46–49], even when the enzyme is near-maximally activated [4,5,7]. In addition, since dichloroacetate did not change mitochondrial respiration, there was no physiologic stimulus for increased PDH flux. Taken together, the glucose/dichloroacetate experiments of Table IV could not support a regulatory or rate-limiting role of the monocarboxylate transporter in the normal and catecholamine-stimulated working guinea-pig heart.

Table IV further shows that dichloroacetate stimulated mitochondrial pyruvate transport (oxidation) regardless of whether the alternative substrate competed for the same monocarboxylate carrier (ketone bodies; series V, VI, VII) or whether they were essentially freely diffusible (octanoate, acetate; series I, II, III, VI, VII). Likewise, stimulation of cardiac work by norepinephrine per se (in the absence of dichloroacetate) to produce the known activation of PDH, was consistently associated with enhanced $^{14}CO_2$ production from [U-^{14}C]glucose or [1-^{14}C]pyruvate and hence prior mitochondrial pyruvate uptake (Table IV, series II–VII). Adrenergic stimulation of pyruvate transport plus oxidation was especially pronounced in presence of β-hydroxybutyrate as the alternative substrate (series V). As for the effects of dichloroacetate, even when pyruvate oxidation rates were in the upper physiologic range due to norepinephrine, dichloroacetate did not fail to further increase $^{14}CO_2$-production from labelled glucose (series II, III) or pyruvate (series IV–VII).

Pyruvate oxidation from glucose during maximum adrenergic stimulation

Table V shows that in the absence of competing exogenous substrate and during maximum stimulation of metabolic rates as well, pyruvate decarboxylation

TABLE V

Work output-related changes in glucose oxidation and specific activity of lactate in perfused guinea-pig hearts utilizing 5 mM [U-^{14}C]glucose (+ 5 U/l insulin) as sole substrate during adrenergic stimulation

Values are means (± S.E.) from quadruple determinations, N, number of working hearts tested under standard load conditions (see Methods). Control data refer to 16–20 min perfusion with [U-^{14}C]glucose. Tracer infusion was then continued for another 32 min, 16 min for each norepinephrine concentration. The catecholamine data refer to steady states of the last 4 min of each respective phase. Except for oxygen uptake (μmol/min per g dry mass) all metabolic rates expressed as μmol C_3/min per g dry mass. [a] Calculated assuming 6 O_2-equivalents for complete oxidation of glucose measured as $^{14}CO_2$ production/(S.A. of ven. lactate). S.A., specific activity (%) relative to that of arterial glucose (dpm/μmol). * $P < 0.03$ by ANOVA relative to respective controls. Relative S.A. of lactate was strictly inversely related to adrenergic stress as measured by oxygen uptake: rel. S.A. = 0.82(±0.03) − 0.0063 (±0.0006) × oxygen uptake, $R^2 = 0.921$; $P < 0.0001$; $n = 13$. NE, norepinephrine; HR·ΔLVP, heart rate-pressure product (cmH_2O/min).

Condition	N	S.A. of ven. lactate (S.A. of glucose = 1)	$^{14}CO_2$ production	$^{14}CO_2$ production/ (S.A. of ven. lactate)	Oxygen uptake	% oxygen uptake for glucose oxidation [a]	HR·ΔLVP
Control	5–8	0.560 ±0.010	10.17 ±0.71	9.12 ±0.68	40.72 ±1.35	67.2 ±0.45	18217 ±381
0.08 μM NE	4	0.449 * ±0.004	14.39 * ±0.20	16.05 * ±0.53	62.85 * ±1.24	76.6 * ±0.02	25531 * ±648
0.50 μM NE	4	0.333 * ±0.003	18.39 * ±0.29	27.66 * ±0.60	74.34 * ±1.26	111.7 * ±2.3	27257 * ±1069

from glucose kept pace with mitochondrial respiration. With glucose as sole substrate, the intracellular pyruvate concentration was lower than normal, 90 μM (cf. Table I series I; [31]). Nevertheless, $^{14}CO_2$ production from [U-^{14}C]glucose, corrected for the specific activity of lactate, accounted for 77% and 112% of myocardial O_2 uptake during prolonged stimulations by low and high doses of norepinephrine, respectively. If mitochondrial transport had become rate-limiting at the high oxidative rates caused by adrenergic stimulation, the glucose-dependent hearts might eventually have developed ventricular failure secondary to blockade of mitochondrial pyruvate uptake and oxidation. Such mechanical failure was observed when α-cyano-4-hydroxycinnamate disabled the carrier in the absence of stabilizing octanoate (data not shown). However, the catecholamine-stimulated hearts of Table V performed at increased or near-maximal heart rate × pressure products (Table V, right column) and ventricular inotropism [6] and pyruvate decarboxylation adjusted readily to enhanced mitochondrial respiration and ventricular work output. This reflected a demand-induced acute upregulation of PDH flux in accordance with the immediate energy requirements of the myocardium.

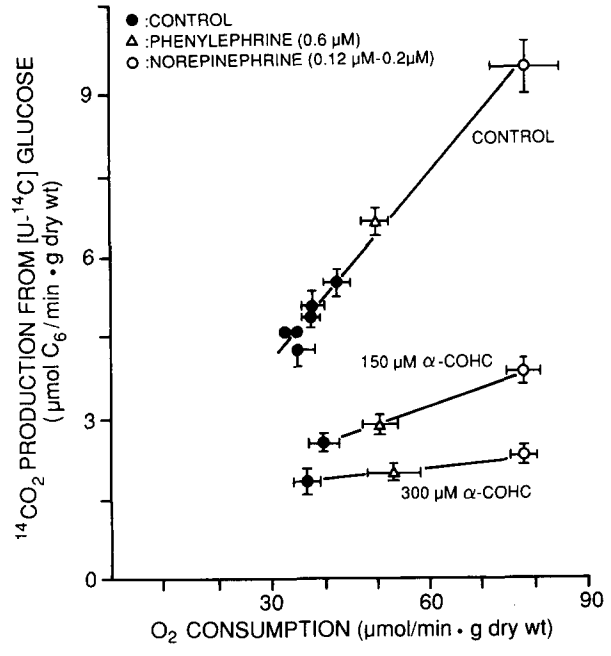

Fig. 4. Dissociation of work-dependent pyruvate oxidation from mitochondrial respiration by α-cyano-4-hydroxycinnamate. The dependence of glucose-derived pyruvate oxidation on ventricular work output was monitored by myocardial O_2 consumption during α- and β-adrenergic stimulations. Hearts metabolized 5 mM [U-^{14}C]glucose (+5 U/l insulin) combined with 0.2 mM octanoate. To account for intracellular dilution of glycolytic pyruvate during adrenergic stimulation, $^{14}CO_2$ production was corrected for specific activity of lactate (see Materials and Methods and Table V). Rates refer to hemodynamic and metabolic steady states attained after 16–20 min infusions of the catecholamines or α-cyano-4-hydroxycinnamate, respectively. Means ± S.E. from 6–8 hearts.

Clearly these data confirm that (short-term) regulation of myocardial pyruvate oxidation was mainly work-related rather than under the control of a low-capacity mitochondrial monocarboxylate carrier.

Dissociation of pyruvate oxidation from mitochondrial respiration by α-cyano-4-hydroxycinnamate

The question arose as to the physiologic role of the mitochondrial monocarboxylate carrier. Fig. 4 shows that the carrier in situ could indeed strongly limit pyruvate oxidation, if disabled by α-cyano-4-hydroxycinnamate (see also Figs. 1 and 2). At 300 μM perfusate α-cyano-4-hydroxycinnamate, pyruvate oxidation was sharply decreased and nearly completely dissociated from ventricular inotropic function at all physiologic levels of mitochondrial respiration. This suggested that sulfhydryl groups on the transport protein to which the cinnamates likely bind (to produce noncompetitive inhibition) are essential for efficient functioning of the carrier [22]. It could therefore be concluded that the specific monocarboxylate carrier is the physiologic mechanism by which the heart mitochondria mediate work- or inotropism-related pyruvate entry into the matrix. The carrier's poor metabolic control strength is plausible in view of its large transport potential ($\approx$ 100 μmol/min) at $S_{0.5}$ values ($\approx$ 120 μM) near physiologic intracellular pyruvate concentrations. Such kinetic characteristics will assure more than adequate transport capacity under many, if not most physiologic conditions.

Acknowledgements

This study was supported by grants to RB from the National Institutes of Health (RO1 HL-37067) and from the Uniformed Services University of the Health Sciences (RO7638). The skillful technical assistance of David Hartman, Darlene Brodie and Eleanora Juriansz is gratefully acknowledged.

References

1 Cooper, R.H., Randle, P.J. and Denton, R.M. (1975) Nature 257, 808–809.
2 Olson, M.S., Dennis, S.C., DeBuysere, M.S. and Padma, A. (1978) J. Biol. Chem. 253, 7369–7375.
3 Hiltunen, J.K. and Hassinen, I.E. (1976) Biochim. Biophys. Acta 440, 377–390.
4 Hiraoka, T., DeBuysere, M. and Olson, M.S. (1980) J. Biol. Chem. 255, 7604–7609.
5 Bünger, R., Permanetter, B., Sommer, O. and Yaffe, S. (1982) Am. J. Physiol. 242, H30–H36.
6 Bünger, R., Permanetter, B. and Yaffe, S. (1983) Pflügers Arch. 397, 214–219.
7 Bünger, R. and Permanetter, B. (1984) Am. J. Physiol. 247, C45–C52.
8 Hansford, R.G. (1987) Biochem. J. 241, 145–151.

9 Hansford, R., Hogue, B., Prokopczuk, A., Wasilewska, E. and Lewartowski, B. (1990) Biochim. Biophys. Acta 1018, 282–286.
10 Moravec, C.S. and Bond, M. (1992) J. Biol. Chem. 267, 5310–5316.
11 Miyata, H., Silverman, H.S., Sollott, S.J., Lakatta, E.G., Stern, M.D. and Hansford, R.G. (1991) Am. J. Physiol. 261, H1123–H1134.
12 Hansford, R.G., Moreno-Sánchez, R. and Lewartowski, B. (1989) Ann. N.Y. Acad. Sci. 573, 240–253.
13 Veech, R.L., Lawson, J.W.R., Cornell, N.W. and Krebs, H.A. (1979) J. Biol. Chem. 254, 6538–6547.
14 Soboll, S. and Bünger, R. (1981) Hoppe-Seyler's Z. Physiol. Chem. 362, 125–132.
15 Bünger, R. and Soboll, S. (1986) Eur. J. Biochem. 159, 203–213.
16 Bünger, R., Mukohara, N., Kang, Y.H. and Mallet, R.T. (1991) Eur. J. Biochem. 202, 913–921.
17 Deuticke, B., Beyer, E. and Forst, B. (1982) Biochim. Biophys. Acta 684, 96–110.
18 Halestrap, A.P., Scott, R.D. and Thomas, A.P. (1980) Int. J. Biochem. 11, 97–105.
19 Halestrap, A.P. and Denton, R.M. (1975) Biochem. J. 148, 97–106.
20 Kang, Y.H., Mallet, R.T. and Bünger, R. (1992) Pflügers Arch. 421, 188–199.
21 Halestrap, A.P. and Armston, A.E. (1984) Biochem. J. 223, 677–685.
22 Halestrap, A.P. (1978) Biochem. J. 172, 377–387.
23 Thomas, A.P. and Halestrap, A.P. (1981) Biochem. J. 196, 471–479.
24 Shearman, M.S. and Halestrap, A.P. (1984) Biochem. J. 223, 673–676.
25 Bünger, R., Sommer, O., Walter, G., Stiegler, H. and Gerlach, E. (1979) Pflügers Arch. 380, 259–266.
26 Mallet, R.T., Kang, Y.H., Mukohara, N. and Bünger, R. (1992) Biochim. Biophys. Acta 1139, 239–247.
27 Whitehouse, S. and Randle, P.J. (1973) Biochem. J. 134, 651–653.
28 Becker, B.F., Bünger, R., Permanetter, B. and Gerlach, E. (1984) Klin. Wochenschr. 62 (suppl. II), 67–75.
29 Mallet, R.T., Hartman, D.A. and Bünger, R. (1990) Eur. J. Biochem. 188, 481–493.
30 Bünger, R., Mallet, R.T. and Hartman, D.A. (1989) Eur. J. Biochem. 180, 221–233.
31 Bünger, R. (1985) Am. J. Physiol. 249, H439–H449.
32 Mowbray, J. and Ottaway, J.H. (1973) Eur. J. Biochem. 36, 369–379.
33 Williamson, J.R. (1966) J. Biol. Chem. 241, 5026–5036.
34 Snedecor, G.W. and Cochran, W.G. (1980) Statistical Methods, 7th Edn., Iowa State University Press, Ames, IA.
35 Paradies, G. and Papa, S. (1977) Biochim. Biophys. Acta 462, 333–346.
36 Spencer, T.L. and Lehninger, A.L. (1976) Biochem. J. 154, 405–414.
37 Bünger, R., Swindall, B., Brodie, D., Zdunek, D., Stiegler, H. and Walter, G. (1986) J. Mol. Cell. Cardiol. 18, 423–438.
38 Poole, R.C., Halestrap, A.P., Price, S.J., Levi, A.J. (1989) Biochem. J. 264, 409–418.
39 Clarke, K., O'Connor, A.J. and Willis, R.J. (1987) Am. J. Physiol. 253, H412–H421.
40 Zweier, J.L. and Jacobus, W.E. (1987) J. Biol. Chem. 262, 8015–8021.
41 He, M.-X., Gorman, M.W., Romig, G.D. and Sparks, H.V. Jr. (1992) J. Mol. Cell. Cardiol. 24, 79–89.
42 Kusuoka, H., Koretsune, Y., Chacko, V.P., Weisfeldt, M.L. and Marban, E. (1990) Circ. Res. 66, 1268–1276.
43 Bergmeyer, H.U. (1974) Methods of Enzymatic Analysis, 2nd Edn., Academic Press, New York.
44 Palmer, T. (1985) Understanding Enzymes, 2nd Edn., Ellishorwood Publishers, Chichester.
45 Idell-Wenger, J.A., Grotyohann, L.W. and Neely, J.R. (1978) J. Biol. Chem. 253, 4310–4318.
46 Kerbey, A.L., Randle, P.J., Cooper, R.H., Whitehouse, S., Pask, H.T. and Denton, R.M. (1976) Biochem. J. 154, 327–348.
47 Hansford, R.G. and Cohen, L. (1978) Arch. Biochem. Biophys. 191, 65–81.
48 Wieland, O.H., Von Funcke, H. and Löffler, G. (1971) FEBS Lett. 15, 295–298.
49 Reinauer, H. and Müller-Ruchholtz, E.R. (1976) Biochim. Biophys. Acta 444, 33–42.